

Nuclear and Neutron Star Radii

S. Schramm*

Argonne National Laboratory, 9700 S. Cass Avenue, Argonne IL 60439, USA

(Dated: October 30, 2018)

Abstract

We investigate the correlation between nuclear neutron radii and the radius of neutron stars. We use a well-established hadronic SU(3) model based on chiral symmetry that naturally includes non-linear vector meson and scalar meson - vector meson couplings. The relative strengths of the couplings modify the nuclear isospin-dependent interactions. We study the dependence of nuclear and neutron star radii on the coupling strengths. The relevance of the results for parity-violating electron-nucleus scattering and the URCA process in neutron stars is discussed.

PACS numbers: 21.60.-n,12.40.-y

*Electronic address: schramm@theory.phy.anl.gov

I. INTRODUCTION

In light of the new and planned radioactive beam facilities the study of neutron-rich nuclei has received increased attention in recent years. Completing the chart of metastable nuclei towards the proton and neutron drip lines is the major goal of the endeavor with important information for the stellar nucleosynthesis. From a theoretical point of view nuclear calculations toward the neutron drip-line are still quite problematic in part due to the rather poor knowledge of the isospin-dependence of the nuclear forces. Without going to extremely neutron-rich nuclei there is another complementary information by studying nuclear properties and the ultimate neutron-rich systems, i.e. neutron stars, in a combined approach. The radius of a neutron star is sensitive to isospin forces and over a significant part of the star the corresponding nuclear densities have values that also occur in atomic nuclei.

A rather sensitive measure for isospin effects in a normal nucleus is its neutron radius compared to the proton radius. In an upcoming experiment at Jefferson Laboratory an accurate measurement of the neutron radius of ^{208}Pb is planned using parity-violating electron scattering [1].

As a basis for studying correlations between the nuclear radii with neutron star radii a theoretical approach has to be employed that covers nuclear structure as well as neutron star calculations in a unified way. Since the properties of neutron stars can change significantly by including hyperon degrees of freedom, a SU(3)-flavor approach is a convenient choice for such an investigation. In order to study the dependence of nuclear and neutron star radii we investigate the variation of the radii by modifying terms that influence the isospin dependence and nuclear skin effects. Here we follow the analysis of [2, 3] where in a Walecka-type model the sensitivity of nuclear and star radii on the coupling strengths between isovector vector mesons and scalar and vector mesons was investigated. As it turns out such an analysis can be done in our approach in a very natural way.

In the following we present a calculation of the radii of neutron stars and the ^{208}Pb proton and neutron radii in a framework that is based on a model constructed from chiral SU_F(3) arguments. The outline of the article is as follows. First in Section II we briefly introduce the general framework of the chiral model looking at several meson interaction terms. Then in section III we discuss the results of the calculation, studying the dependence of neutron

star radii and nuclear neutron skins on the various coupling constants. From those results we derive the direct correlation between neutron skin and neutron star radius. As a test of our model we also look at the proton skin of proton-rich argon isotopes. Finally, we investigate the consequence for neutron star cooling via the URCA process.

II. THEORETICAL FRAMEWORK

In our nuclear structure as well as in the neutron star calculation we adopt a generalized flavor-SU(3) $\sigma - \omega$ type model. The reason for adopting this model is two-fold. For one it includes, by construction, a nonlinear coupling of the ρ and ω meson as well as coupling between the vector mesons and scalar mesons, so there is no need to add additional terms to an established model to study the type of isospin dependencies mentioned before. Secondly, in addition to successful applications in one- and two-dimensional nuclear structure calculations [4, 5], the same model also shows a sensible behavior at high temperatures and densities[6], which is quite important in this discussion as the inclusion of nonlinear terms in a calculations involving matter in extreme regions of temperature or density, has the general problem that this can produce rather uncontrolled extrapolations. A phenomenological check of the soundness of the model predictions at extreme values is therefore reassuring. The model used here has been successfully tested in all those regimes.

The model includes the complete set of the lowest SU(3) multiplets of baryons and mesons. In addition extensions to higher multiplets have been discussed [7].

Restricting ourselves to those degrees of freedom relevant for the discussion in this paper the general $SU(3)$ Lagrangian [8] reduces to the following structure: The interaction term of baryons, mesons, and the photon reads

$$\mathcal{L}_{int} = - \sum_i \bar{B}_i \left[g_{i\omega} \omega_0 \gamma_0 + g_{i\rho} \tau_3 \rho_0^0 \gamma_0 + \frac{1}{2} e(1 + \tau_3) A_0 \gamma_0 + m_i^* \right] B_i \quad (1)$$

where now the SU(3) baryon octet B is reduced to the isospinor $(\begin{smallmatrix} p \\ n \end{smallmatrix})$. The various coupling constants of mesons and baryons result from the $SU(3)$ structure [8] and the interaction of the scalar fields follows as

$$\begin{aligned} \mathcal{L}_0^{\text{chi}} = & -\frac{1}{2} k_0 \chi^2 (\sigma^2 + \zeta^2 + \delta^2) + k_1 (\sigma^2 + \zeta^2 + \delta^2)^2 + k_2 \left(\frac{\sigma^4}{2} + \frac{\delta^4}{2} + 3\sigma^2\delta^2 + \zeta^4 \right) \\ & + k_3 \chi \sigma^2 \zeta - k_4 \chi^4 - \frac{1}{4} \chi^4 \ln \frac{\chi^4}{\chi_0^4} + \epsilon \chi^4 \ln \frac{(\sigma^2 - \delta^2)\zeta}{\sigma_0^2 \zeta_0} \end{aligned} \quad (2)$$

Here the various scalar fields σ , δ , and ζ correspond to the non-strange isoscalar (σ), isovector (δ) quark-antiquark states, and the strange anti-strange state (ζ). The field χ is the scalar, isoscalar glueball field χ introduced in [9, 10]. χ_0 , σ_0 and ζ_0 ($\delta_0 = 0$) denote the vacuum expectation values of the fields, which are generated via spontaneous symmetry breaking.

The term

$$\mathcal{L}_{ESB} = - \left(\frac{\chi}{\chi_0} \right)^2 [x\sigma + y\zeta] \quad (3)$$

introduces explicit chiral SU(3) symmetry breaking. The coupling strengths are $x = m_\pi^2 f_\pi$ and $y = \sqrt{2}m_K^2 f_K - \frac{1}{\sqrt{2}}m_\pi^2 f_\pi$. f_π and f_K are the pion and kaon decay constant, respectively. The vector meson self-interaction terms have the structure

$$\mathcal{L}_{vec,NL} = -a (\text{Tr} [V^\mu V_\mu])^2 - b \text{Tr} [(V^\mu V_\mu)^2] \quad (4)$$

where V denotes the 3x3 matrix of the vector meson multiplet. In the case of nuclei this reduces to the form

$$\mathcal{L}_{vec} = -g_4^4 (\omega^4 + 6\beta\omega^2\rho^2 + \rho^4) + \dots \quad (5)$$

with the zeroth components of the isoscalar ω and neutral isovector ρ field. The couplings g_4^4 and β are related to a, b of equation 4 via

$$g_4^4 = a/2 + b \quad , \quad \beta = 1 - \frac{2}{3(1 + a/2b)} \quad (6)$$

In addition the vector mesons interact with the glueball field χ and the nonet of scalar mesons Σ via

$$\mathcal{L}_{vs} = c\chi^2 \text{Tr}[V^\mu V_\mu] + d \text{Tr}[\Sigma^2 V^\nu V_\nu] \quad (7)$$

which reduces to

$$\mathcal{L}_{vs} = [c\chi^2 + 2d(\sigma^2 + \delta^2)] (\omega^2 + \rho^2) + \dots \quad (8)$$

In the numerical calculation we investigate the relative strength of the two couplings of the vector mesons to the glueball field as well as to the scalars by varying the quantity r_σ defined as

$$\mathcal{L}_{vs} = \frac{\alpha}{(1 - r_\sigma)\chi_0^2 + r_\sigma\sigma_0^2} [(1 - r_\sigma)\chi^2 + r_\sigma(\sigma^2 + \delta^2)] (\omega^2 + \rho^2) \quad (9)$$

where the factor α was determined in the general parameter fit χ_M with $r_\sigma = 0$ [4]. r_σ shifts the relative importance of the gluonic and quark-type scalar fields for generating the masses of the vector mesons. The mass of the baryons are dynamically generated via their

interaction with the scalar fields following Eq. (1), which automatically leads to density and temperature-dependent masses. Explicitly, the baryon masses m_i^* are given by

$$m_i^* = g_{i\sigma}\sigma + g_{i\delta}\delta + g_{i\zeta}\zeta \quad . \quad (10)$$

In general there is no unique way of introducing nonlinear vector couplings in a hadronic model. Here we introduce the simplest structures within our framework generating the interaction terms, in fact those terms had been introduced well before this specific investigation of isospin effects started. The non-linear couplings in the ω channel turn out to be very important to obtain a reasonably soft equation of state of symmetric nuclear matter, leading to acceptable value for the compressibility of $\kappa < 250$ MeV. In addition, away from the saturation density the equation of state of neutron matter is soft enough to generate neutron stars with masses $M < 2M_{solar}$ [11].

III. RESULTS

A. Neutron skins

Here we show the numerical results obtained by solving the equations of motions derived from the Lagrangian terms discussed above in a mean field approximation. In particular we will vary the two coupling strengths β , Eq. (5), and r_σ , Eq. (9) and study their influence on various observables.

First we determine the rms radii of neutrons and protons in ^{208}Pb . In addition as comparison we also look at the case of the singly magic ^{138}Ba which might be of interest in future parity-violation experiments. Barium isotopes have been suggested as candidates for atomic parity violation experiments [13] in analogy to the cesium experiments [14]. In those experiments uncertain neutron distributions are a major part of the theoretical error. The calculation of ^{138}Ba is supposed to give an idea of the range of uncertainty for neutron skins in barium.

The equation of motions are solved assuming spherical symmetry using the established parameter set χ_M [4]. The calculation is repeated by changing the two coupling parameter β and r_σ . The resulting values for the difference of proton and neutron radii $\Delta r_{np} \equiv r_n - r_p$ are shown in Figure 1. In the variation of the parameters we follow two general procedures. First we use the parameters χ_M and only modify the coupling strength β (which has a

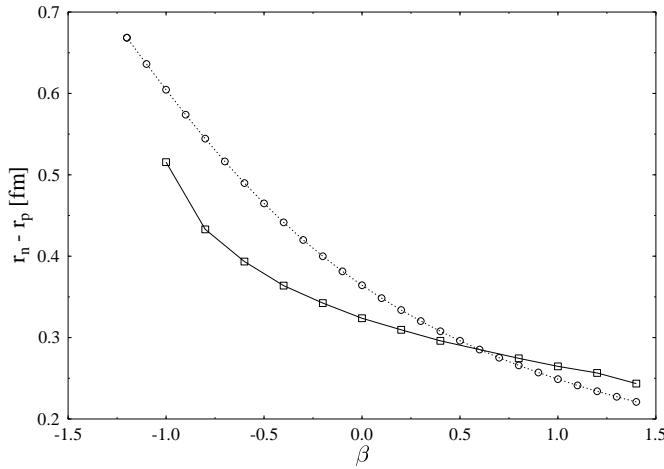


FIG. 1: Difference of neutron and proton radius in ^{208}Pb as function of nonlinear vector coupling strength β with (squares) and without (circles) refitting of parameters ($r_\sigma = 0$).

value $\beta = 1$ in χ_M), without simultaneously modifying any other parameters. In a second run we adjust the other parameters that mainly influence the isospin behavior, g_4^4 and the nucleon-rho coupling $g_{N\rho}$ to ensure a correct description of the lead charge radius and binding energy. The result of both approaches is shown in the figure. The general behavior is the same for both approaches. The best-fit estimate for neutron-proton radius difference is $\Delta r_{np} = 0.25$ fm. This number is in general agreement with other models based on relativistic descriptions of nuclear matter [15] and is bigger than typical Skyrme-based non-relativistic projections of $\Delta r_{np} < 0.2$ fm [16]. There is a significant dependence of Δr_{np} on the coupling strength while varying β between about $-1 < \beta < +1.4$, which is about the maximum range in which one can obtain stable nuclear solutions. We will look at the parameter range in more detail. In order to obtain a more believable quantitative result a refitting of the parameters is necessary, reducing Δr_{np} by up to 20 percent. In the following, if not noted otherwise, we will always perform a readjustment of the parameters as explained above. Figure 2 shows results for Δr_{np} varying the coupling r_σ for different values of β . The shaded area reflects the expected accuracy of the neutron radius measurement of about $\pm 1\%$. Note the wiggle for the line with $\beta = 1.4$, signalling the onset of proton and neutron rearrangements

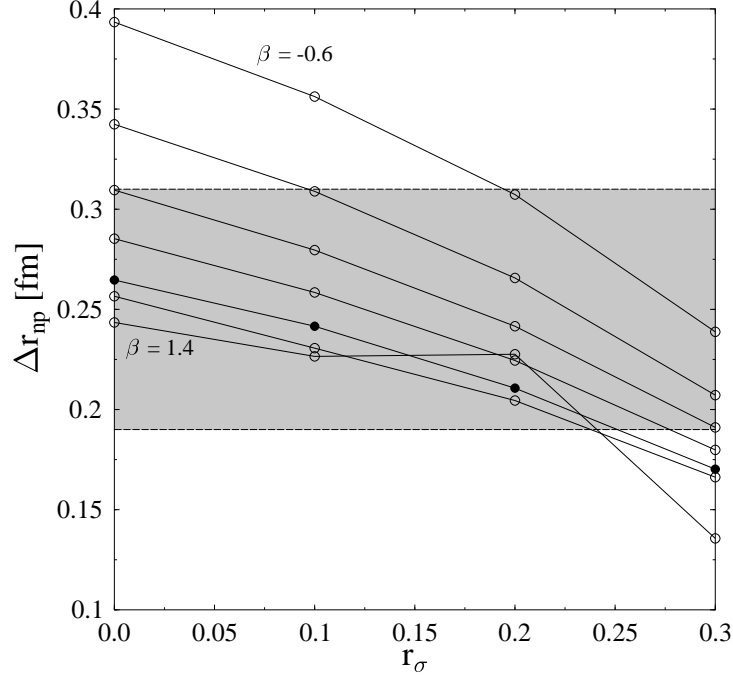


FIG. 2: Difference of neutron and proton radius Δr_{np} in ^{208}Pb as function of relative vector-scalar meson coupling strength r_σ for different values of $\beta = \{-0.6, -0.2, 0.2, 0.6, 1.0, 1.2, 1.4\}$. The shaded area denotes the expected experimental accuracy for the r_n measurement (tentatively) centered at $\Delta r_{np} = 0.25 \text{ fm}$.

in the solutions of the nuclear equations that violate experimentally known nuclear charge distributions.

We repeat the same calculation for the case of ^{138}Ba , Fig. 3. The results are essentially similar. The dependence of the neutron skin is somewhat less pronounced compared to the lead case.

B. Nuclear matter

In order to check that aside from a reasonable description of ^{208}Pb the range of parameter values yields adequate behavior of nuclear matter at saturation we study the values for the

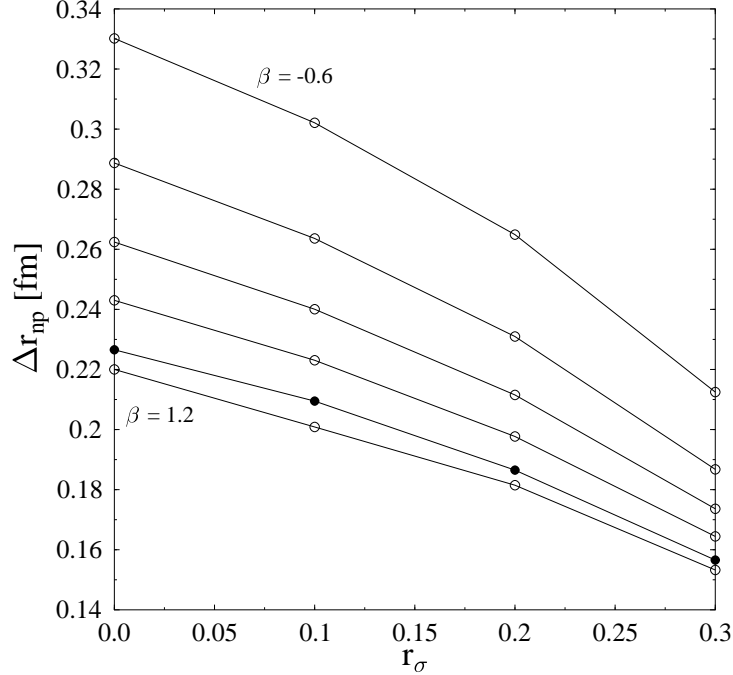


FIG. 3: Difference of neutron and proton radius in ^{138}Ba as function of coupling strength r_σ . Curves for different values of $\beta = \{-0.6, -0.2, 0.2, 0.6, 1.0, 1.2\}$ are shown (cf. Fig. 2).

compressibility κ and the asymmetry energy a_4 at saturation density ρ_0 , which has a value $\rho_0 \sim .15 \text{ GeV/fm}^3$ for all studied parameter sets. κ and a_4 are defined as

$$\kappa = 9\rho_0^2 \frac{\partial^2(E/A)}{\rho^2} \Big|_{\rho=\rho_0}, \quad a_4 = \frac{\rho_0^2}{2} \frac{\partial^2(E/A)}{\partial(\rho_n - \rho_p)^2} \Big|_{\rho=\rho_0} \quad (11)$$

Fig. 4 shows the r_σ dependence of κ . The two curves correspond to two extreme values of β , the other results lie between these curves. Given these numbers one cannot exclude any parameters within the range under consideration, all give reasonable values for the compressibility of nuclear matter between about 205 and 225 MeV. The results for the asymmetry energy are more restrictive. Assuming that acceptable value for the asymmetry should be somewhere between 28 and 38 MeV, values of r_σ larger than 0.2 yield asymmetries a_4 that are too small, whereas given small couplings of scalar and vector mesons the coupling term β should be larger than 0. However, a quite large range of reasonable parameter values

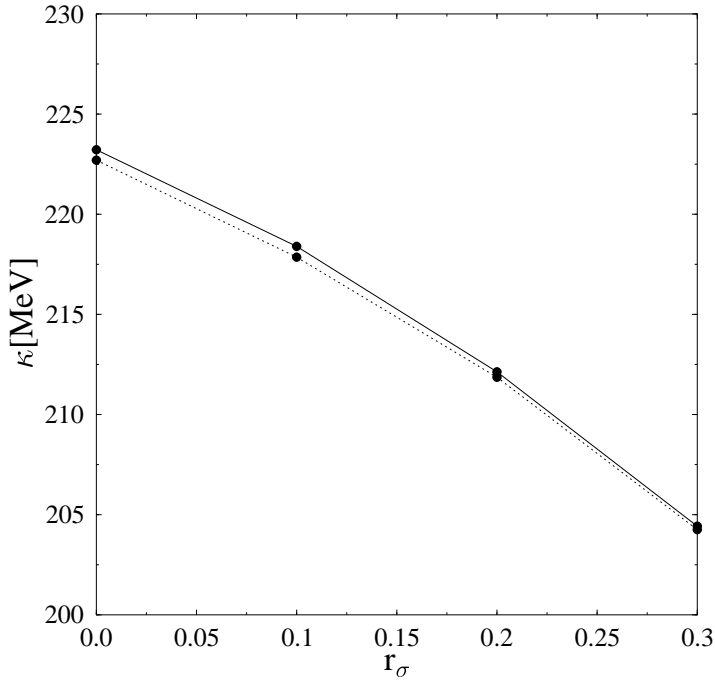


FIG. 4: Results for the compressibility κ as function of the coupling strength r_σ . The two curves show the results for the different values of $\beta = 1.2$ (full line) and $\beta = -0.6$ (dotted line).

persists.

C. Neutron stars

As a complementary source of information on the isospin-dependence of nuclear forces a neutron star probes the extreme neutron-rich system with a content of about 90% neutrons of all baryons in the star. We have performed calculations of neutron star properties in this model before in [11, 12]. The calculation is done by integrating the Tolman-Oppenheimer-Volkov (TOV) equations [17] for the star given an equation of state $\epsilon(P)$ generated from the model Lagrangian:

$$\frac{dP(r)}{dr} = -\frac{(\epsilon+P)(4\pi r^3 P + m)}{r^2(1-2m(r)/r)} \quad (12)$$

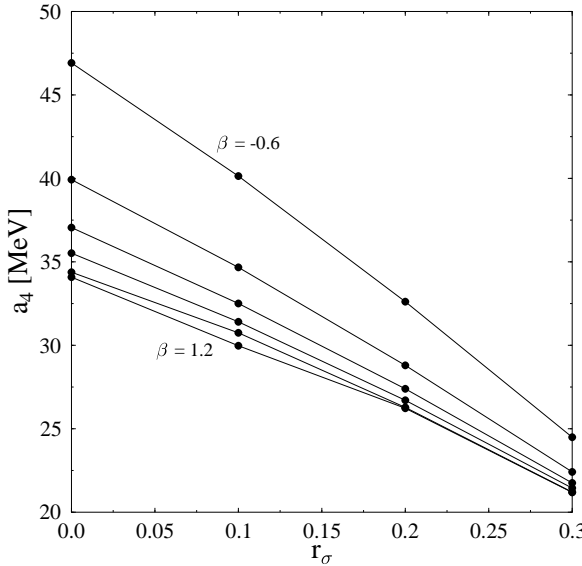


FIG. 5: Results for the asymmetry energy a_4 of saturated nuclear matter as function of the coupling strength r_σ . The horizontal axis shows the value for r_σ whereas the different curves are distinguished by their values of β ranging from -0.6 to 1.2 (see Fig. 3).

$$\frac{dm(r)}{dr} = 4\pi r^2 \epsilon(r) , \quad (13)$$

where P and ϵ are the pressure and energy density of the nuclear matter. $m(r)$ is the gravitational mass of the star inside of the radius r . By fixing the initial value for the pressure P_c in the center of the star, with the knowledge of the equation of state $\epsilon_c(P_c)$ one can integrate equations (12) and (13) from the center of the star outward to the point of vanishing pressure, which defines the star radius R . The calculation of $\epsilon(P)$ is discussed in detail in [6]. The outer crust of the neutron star is modelled as discussed in [11].

Figure 6 shows the resulting neutron star radii for a typical neutron star with a mass of 1.4 solar masses. As in the nuclear case we checked for the consequences of refitting the parameters. But in this case the refitting does not affect the neutron star properties appreciably as can be inferred from the figure. There is a strong dependence of the neutron star radius on the coupling strength with a variation of about 5.5 km over the whole range of values for β that yield reasonable nuclei. However, with reference to the results for the

asymmetry shown in Fig. 5 in this case for $r_\sigma = 0$ β should be chosen to be larger 0, which limits the variation of the star radius to about 1 km. Another uncertainty entering the theoretical determination of neutron star radii comes from the treatment of the hyperons in the star. Although our model is based on a SU(3) model and therefore automatically contains hyperons (Λ , Σ and Ξ baryons, see [11] for a detailed discussion), due to the poor knowledge of the behavior of hyperons in dense matter, results might vary with the treatment of the hyperon sector. To check the limit of the uncertainties we switch off (by hand) the hyperon densities and repeat the radius calculations for the example of the best-fit parameter set χ_M . The variation for a 1.4 solar mass star, $R_{hyper} = 11.42$ km and $R_{nohyper} = 12.46$ km is of the same order as the variation due to the meson-meson couplings. So in addition to a good knowledge of the nuclear isospin forces some information on hyperons in matter is needed to draw more reliable conclusions from neutron star radius data.

A complete set of correlations between Δr_{np} and R_{ns} is given in Fig. 7. The various lines are results for different choices of β and show the dependence on the scalar-vector meson coupling r_σ . The result shows that the information contained in β and r_σ is rather complementary. Whereas the star radius largely depends on β and little on r_σ in the case of the neutron skin the result is the opposite, a strong r_σ dependence and a small influence from the β value. However, as can be seen from the hatched area a 1% measurement of the neutron radius of lead covers about the whole range of results except for very small β and large r_σ values which are largely excluded by the results for the asymmetry energy.

D. Additional tests

As a cross check to our discussion we looked at the proton skin in different isotopes of argon. The skin was experimentally deduced by combining measurements of heavy-ion reaction cross sections[18] with atomic isotope shift data [19]. The resulting values, with rather large error bars, are shown in Figure 8, compared to the theoretical calculations using the same model for several values of the nonlinear coupling varying β (r_σ is set to 0). One can see that with the exception of the point at the high-end of coupling strengths for the ^{32}Ar isotope the agreement with data is quite good, independent of the β parameter. This gives some confidence in the analysis that a change of the coupling does not automatically lead to distorted results of other isospin-related observables.

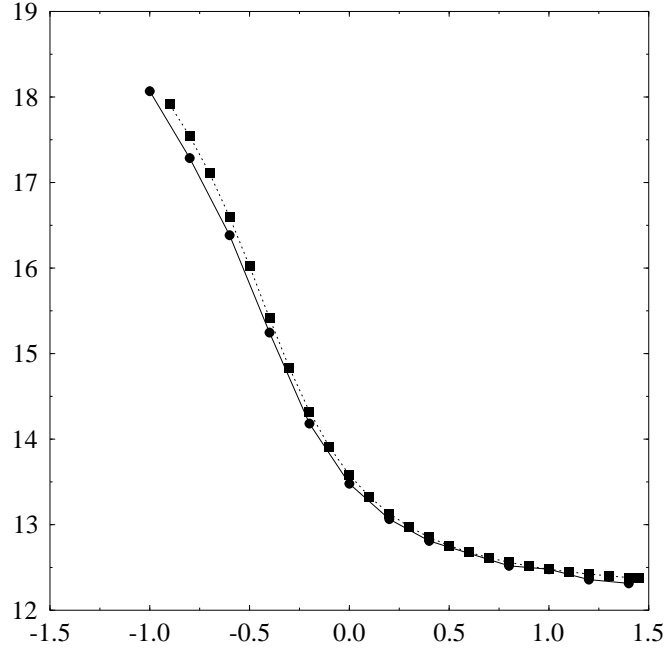


FIG. 6: Radius of a neutron star with $M = 1.4 M_{solar}$ varying the nonlinear coupling strength β for a fixed $r_\sigma = 0$. The solid (dashed) line shows the results with (without) refitted parameters (see text).

Finally, in [20] the importance of the URCA process for neutron star cooling was discussed in this context. The URCA process is thought to be an important mechanism for cooling the neutron star after the supernova explosion at reasonably fast rates in agreement with astronomical observations. This is done via the process $n \rightarrow p + e^- + \bar{\nu}_e$ where the neutrino escapes and carries energy away from the system. This process can proceed when the fermi momenta of the particles involved match :

$$p_n^F \leq p_p^F + p_e^F \quad (14)$$

Thus for the URCA process to take place one needs a significant amount of protons of roughly 11% in the system. As the proton to neutron ratio in the star is influenced by the isospin-dependence of the nuclear forces one has to check whether changing the force

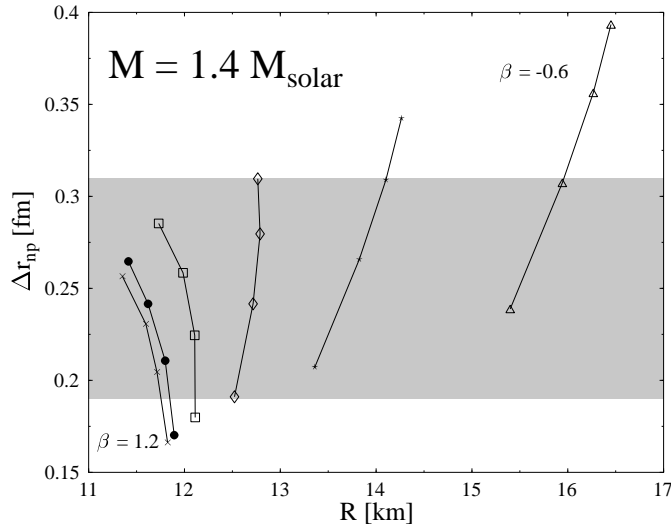


FIG. 7: Relation of the difference of neutron and proton radius Δr_{np} of ^{208}Pb (full symbols) and the neutron star radius ($M = 1.4 M_{\text{solar}}$). The coupling strengths β and r_σ are varied. Results for different values of β are marked with different symbols with values of 1.2, 1.0 0.6, 0.2, -0.2, -0.6 from the left to the right. For every value of β we varied r_σ between 0 and 0.3, with large values of r_σ yielding small values of Δr_{np} as can also be seen in Fig. 2.

might switch off the URCA process. We again consider a 1.4 solar mass star and compare the central density of the star with the minimum density for the URCA process to occur according to equation 14. We see from Figure 9 that the minimum density is always reached. Thus the discussion of the correlation of the star radius and neutron skin is not affected by additional constraints from neutron star cooling considerations.

IV. CONCLUSION

We studied the influence of couplings between vector and scalar mesons as well as non-linear vector-meson interactions and their influence on isospin-related observables following the discussion in [3] (see also [21]). As basic model for our calculation we used a chiral $\sigma - \omega$ type SU(3) model. This model has the benefits of including those nonlinearities from

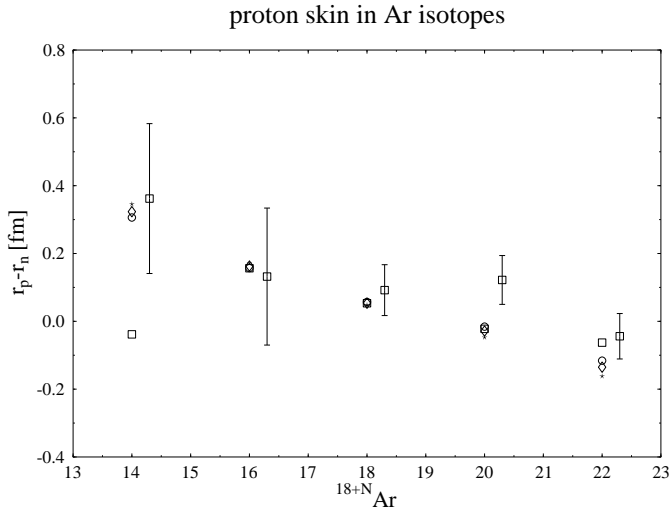


FIG. 8: Proton skin for various Argon isotopes in comparison to experimental values [18]. Results for different nonlinear coupling strengths are shown, the squares, circles, diamonds and stars mark results for $\beta = 1.4, 1.0, -0.2, -0.6$, respectively.

the start and implements them in a rather general SU(3) coupling scheme. Our model has been successfully employed in nuclear structure calculations and in calculations involving high-density and high-temperature environments. Since we also study neutron stars the benefit of having an SU(3) model is that hyperons are automatically included in the model which is quite important for getting reasonably small neutron star masses in accordance with observation. The results show clear dependence of the neutron skin in lead and barium on couplings of vector and scalar mesons, whereas the neutron star radii depend largely on non-linear terms in the vector-meson channel. There is a distinct correlation of neutron star radii and neutron distributions in nuclei as has already been observed in other nuclear structure models [2, 3]. However, although the upcoming measurements of the lead radius using parity-violating electron scattering experiments certainly will give additional information for modelling the isospin-sector of the nuclear forces, it is likely not stringent enough to nail down the parameters. Also possible measurements of neutron star radii can only be useful in this regard if the accuracy of the radius measurement is well below 1 km. At this level of radius uncertainty also the detailed treatment of the hyperons in the neutron star

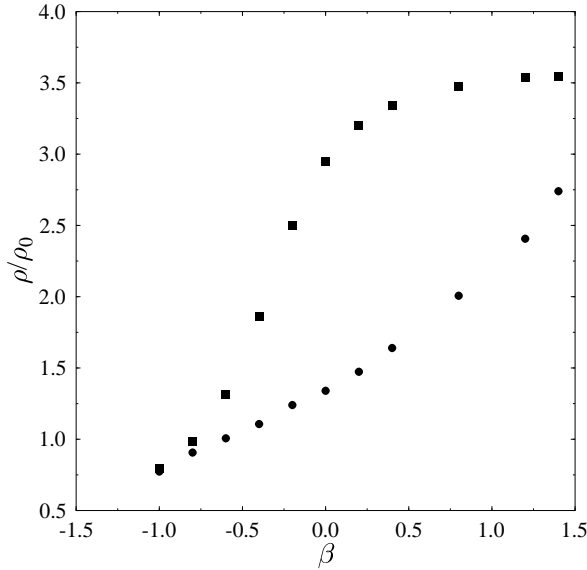


FIG. 9: Critical density for the onset of the URCA process for different nonlinear coupling strengths β setting $r_\sigma = 0$. The squares show the maximum density for a neutron star with a typical mass of $M = 1.4 M_{solar}$. The circles represent the minimum density necessary for the URCA process.

enter, which will make it very difficult to disentangle the different effects on the star radius.

To complete our investigation we have shown that the requirement of fast neutron star cooling does not constrain this discussion. Also the measured value of the proton skins of argon isotopes can be reproduced and are not strongly affected by varying the nonlinear couplings.

Acknowledgments

This work was supported by the U.S. Department of Energy, Nuclear Physics Division (Contract No. W-31-109-Eng-38).

[1] JLab experiment E-00-003, R. Michaels, P.A. Souder, G.M. Urciuoli (spokespersons)

- [2] C. J. Horowitz and J. Piekarewicz, Phys.Rev. C64, 062802 (2001).
- [3] C. J. Horowitz and J. Piekarewicz, Phys.Rev.Lett. 86, 5647 (2001).
- [4] S. Schramm, preprint nucl-th/0207060, Phys. Rev. C. to be published.
- [5] Ch. Beckmann, P. Papazoglou, D. Zschiesche, S. Schramm, H. Stöcker, and W. Greiner, Phys. Rev. C **65**, 024301 (2002)
- [6] D. Zschiesche, P. Papazoglou, S. Schramm, J. Schaffner-Bielich, H. Stoecker, and W. Greiner, Phys.Rev. C63 (2001) 025211.
- [7] D. Zschiesche, S. Schramm, J. Schaffner-Bielich, H. Stoecker, W. Greiner, preprint nucl-th/0209022, to be published in Phys. Lett. B.
- [8] P. Papazoglou, D. Zschiesche, S. Schramm, J. Schaffner-Bielich, H. Stöcker, W. Greiner, Phys. Rev. **C59**, 411 (1998).
- [9] J. Schechter, Phys.Rev. D21, 3393 (1980).
- [10] P. Papazoglou, S. Schramm, J. Schaffner-Bielich, H. Stcker, and W. Greiner, Phys.Rev. C57, 2576 (1998).
- [11] M. Hanuske, D. Zschiesche, S. Pal, S. Schramm, H. Stöcker, and W. Greiner, Ap. J. 537, 958 (2000).
- [12] S. Schramm and D. Zschiesche, preprint nucl-th0204075, submitted to J. Phys. G.
- [13] M. J. Ramsey-Musolf, Phys. Rev. C60 (1999) 015501.
- [14] S. C. Bennett and C. E. Wieman, Phys. Rev. Lett. **82**, 2484 (1999).
- [15] D. Vretanar, G. A. Lalazissis, and P. Ring, Phys. Rev. C 62, 045502 (2000).
- [16] K. Pomorski, P. Ring, G.A. Lalazissis, A. Baran, Z. Lojewski, B. Nerlo-Pomorska, and M. Warda, Nucl.Phys. A624, 349 (1997).
- [17] R.C. Tolman, Phys. Rev. 55 (1939) 364;
J.R. Oppenheimer and G.M. Volkoff, Phys. Rev. 55 (1939) 374.
- [18] A. Ozawa et al., preprint RIKEN-AF-NP-424, May 2002.
- [19] A. Klein et al., Nucl. Phys. **A607**, 1 (1996).
- [20] C. J. Horowitz and J. Piekarewicz, preprint nucl-th/0207067 (2002).
- [21] A. R. Bodmer and Q. N. Usmani, Argonne preprint (2002).